

Grafted Metallocalixarenes as Single-Site Surface Organometallic Catalysts

Justin M. Notestein, Enrique Iglesia, and Alexander Katz*

Contribution from the Department of Chemical Engineering,
University of California at Berkeley, Berkeley, California 94720-1462

Received May 20, 2004; E-mail: katz@cchem.berkeley.edu

Abstract: Metallocalixarenes were grafted onto silica using a surface organometallic approach and shown to be active and selective catalysts for epoxidation of alkenes using organic hydroperoxides. Calixarene–Ti^{IV} precursors were anchored at surface densities from 0.1 to near-monolayer coverages (0.025–0.25 calixarene nm⁻²). Several spectroscopic methods independently detected calixarene–Ti^{IV} connectivity before and after epoxidation catalysis. Kinetic analyses of cyclohexene epoxidation confirmed that the active sites were anchored on the silica surface and were significantly more active than their homogeneous analogues. The steric bulk and multidentate binding of the calixarenes led to structural stability and to single-site behavior during epoxidation catalysis. Rate constants were independent of surface density for cyclohexene epoxidation with *tert*-butyl hydroperoxide (11.1 ± 0.3 M⁻² s⁻¹) or cumene hydroperoxide (25 ± 2 M⁻² s⁻¹). The materials and methods reported here allow the assembly of robust surface organometallic structures in which the active sites behave as isolated species, even near saturation monolayer coverages. In turn, this makes possible the rational design and synthesis of a class of heterogeneous oxide catalysts with atomic-scale precision at the active site.

Introduction

Many heterogeneous catalysts currently in practice are chemically complex and consist of oligomeric active site structures that are difficult to optimize via atomic-scale control at the active site. A promising new method for the design and synthesis of heterogeneous catalysts with control of active site structure involves the use of emerging concepts in surface organometallic chemistry. Surface organometallic catalysts consist of a transition-metal-containing active site that is grafted onto a solid support, which serves as a rigid ligand for the metal center.^{1–5} These catalysts can exhibit interesting support effects, including large rate enhancements, when active sites are anchored onto supports instead of acting as homogeneous entities in solution.^{2,3} These rate enhancements resemble those reported for systems consisting of hybrid organic–inorganic materials,⁶ and reflect the synergy between the catalytically active site and a support surface that acts as a ligand.

We report here a new strategy to control the interplay between metal centers and organic ligands or surfaces in grafted organometallic catalysts. Our approach involves confining an isolated metal atom within a pseudotetrahedral oxo coordination

environment, defined from the top by a calixarene molecule and from the bottom by a silica surface. The rigidity and steric bulk of both ligands—calixarene and silica—ensure metal atom site isolation, even during kinetic processes that require ligand exchange; such stability is essential for durable and robust heterogeneous catalysts.

Our synthesis of grafted metallocalixarene catalysts is based on anchored calixarene structures **1** and **2**. These have been synthesized according to previously reported procedures by treating a calixarenetriol or -tetrol compound with an activated silica containing chloride ligands.⁷ We previously showed that this process leads to the grafting of a calixarene monolayer and to a 10 Å decrease in the average pore radius of the silica support, consistent with the expected thickness of a single calixarene layer. Each calixarene in **1** was shown to act as a stoichiometric adsorbent for one toluene molecule, a result that is consistent with an open cone conformer for each anchored calixarene.⁷

Koiland molecules⁸ originally inspired the synthesis of grafted calixarenes **1** and **2**. Reports of isostructural Ti dimers of calixarenes,⁹ as well as structures in which calixarenes serve as a well-defined oxo surface for several other metals,¹⁰ suggested to us that the Si atom in **2** could be successfully replaced by transition metals of catalytic interest. We report

(1) Copéret, C.; Chabanas, M.; Saint-Arroman, R. P.; Basset, J. M. *Angew. Chem., Int. Ed.* **2003**, *42*, 156–181.

(2) Atfield, M. P.; Sankar, G.; Thomas, J. M. *Catal. Lett.* **2000**, *70*, 155–158.

(3) Meunier, D.; Piechaczyk, A.; de Mallmann, A.; Basset, J. M. *Angew. Chem., Int. Ed.* **1999**, *38*, 3540–3542.

(4) Jarupatrakorn, J.; Tilley, T. D. *J. Am. Chem. Soc.* **2002**, *124*, 8380–8388.

(5) Bouh, A. O.; Rice, G. L.; Scott, S. L. *J. Am. Chem. Soc.* **1999**, *121*, 7201–7210.

(6) Bass, J. D.; Anderson, S. L.; Katz, A. *Angew. Chem., Int. Ed.* **2003**, *42*, 5219–5222.

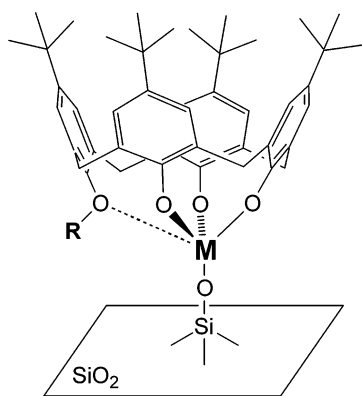
(7) Katz, A.; Da Costa, P.; Lam, A. C. P.; Notestein, J. M. *Chem. Mater.* **2002**, *14*, 3364–3368.

(8) Delaigue, X.; Hosseini, M. W.; de Cain, A.; Fischer, J. *Tetrahedron Lett.* **1993**, *34*, 3285–3288.

(9) Olmstead, M. M.; Sigel, G.; Hope, H.; Xu, X.; Power, P. P. *J. Am. Chem. Soc.* **1985**, *107*, 8087–8091.

(10) Floriani, C.; Floriani-Moro, R. *Adv. Organomet. Chem.* **2001**, *47*, 167–233.

here the Ti analogue **3** of material **2**. Material **3** is based on molecular precursor **4b**, which has been synthesized and characterized using single-crystal X-ray diffraction.¹¹



- 1**, M = Si, R = H
2, M = Si, R = CH₃
3, M = Ti, R = CH₃

Our objective in substituting Ti within the grafted metallocalixarene architecture is to incorporate epoxidation catalytic activity in the same manner as for titanium silicalite (TS-1), in which isolated Ti atoms replace Si atoms within the zeolite framework.^{12–14} We demonstrate the utility of **3** as a highly active, stable, and selective catalyst for alkene epoxidation. Grafted titanium complexes catalyze epoxidation reactions but lose activity and selectivity during catalysis, especially at high surface Ti loadings, which fail to maintain metal site isolation and tend to form Ti–oxo oligomers.^{15–17} Some previous attempts to combine organic and inorganic ligands around Ti metal centers have led to more active catalysts, but also to sterically hindered sites, leaching, or ligand exchange during epoxidation catalysis.^{2,4,18–20} We show here that material **3** is active and stable during epoxidation catalysis and shows single-site catalytic behavior. These conclusions are supported by spectroscopic characterization and measurements of intrinsic epoxidation rate constants on **3**; these rate constants are large and do not change with reaction time or Ti surface density.

The type of grafted metallocalixarene material reported here for Ti active species is directly extendable to other transition metals and to the synthesis of isolated active sites for a wide range of chemical transformations. Also, because of their single-site nature, these materials provide robust strategies for optimizing catalyst activity and selectivity via calixarene ligand design and synthesis, which exploit the existing diversity and flexibility of metallocalixarene synthetic chemistry.^{10,21} We anticipate broad utility for grafted metallocalixarenes as new surface organometallic catalysts and as a powerful platform for improv-

ing existing heterogeneous catalysts and elucidating their catalytic mechanisms.

Experimental Section

Precursor Synthesis. Calixarene–Ti^{IV}Cl **4b** was prepared by refluxing 1.0 equiv of dimethoxycalixarene **5a** (Acros, 99%) with TiCl₄ in toluene (Aldrich, 1.0 M) for 48 h followed by recrystallization from hexane according to previously published procedures.¹¹ Elemental analysis (Anal. Calcd for **4b**·(C₇H₈)_{0.5}: C, 73.79; H, 7.55. Found: C, 73.97; H, 7.82) and ¹H NMR (400 MHz, CDCl₃, 298 K) (δ 1.21 (m, 36H, Bu^t), 3.34 (dd, 4H, *J* = 12.4 Hz, *exo*-CH₂), 4.23 (s, 3H, OCH₃), 4.35 (d, 2H, *J* = 12.4 Hz, *endo*-CH₂), 4.78 (d, 2H, *J* = 12.4 Hz, *endo*-CH₂), 7.05 (m, 8H, ArH)) agreed with published values. The four doublets in the methylene region are characteristic of the lower symmetry of the mono-demethylated product **4b**. Calixarene **5a** has only two methylene doublets. Species **4b** could be stored for several weeks as a dark red toluene solution under Schlenk conditions without detectable degradation.

Immobilization of 4b To Yield 3-75. In the naming scheme used here, **3-75** indicates a material with 75 μmol of calixarene–Ti^{IV} per g of catalyst. Chromatography silica gel (300 mg, 60 Å pores, 250–500 μm, Selecto) was partially dehydroxylated under dynamic vacuum at 500 °C for 24 h. The silica was transferred to a flask with 50 mL of anhydrous toluene. A 25 μmol sample of **4b** (as a toluene solution) was added and the suspension refluxed under N₂. The red color of **4b** was gradually transferred from the solution to the solid. After 0.5 h, 70 μL of 2,6-di-*tert*-butylpyridine (0.25 mmol) was added, and the suspension was returned to reflux. After 24 h, the solid was filtered, washed with ~300 mL of hot anhydrous toluene, and dried under dynamic vacuum at 25 °C for at least 4 h and at 250 °C for 1 h. Materials with identical catalytic behavior were made with and without recrystallization of **4b**, thus enabling the entire catalyst synthesis to occur in a single pot using commercially available reagents.

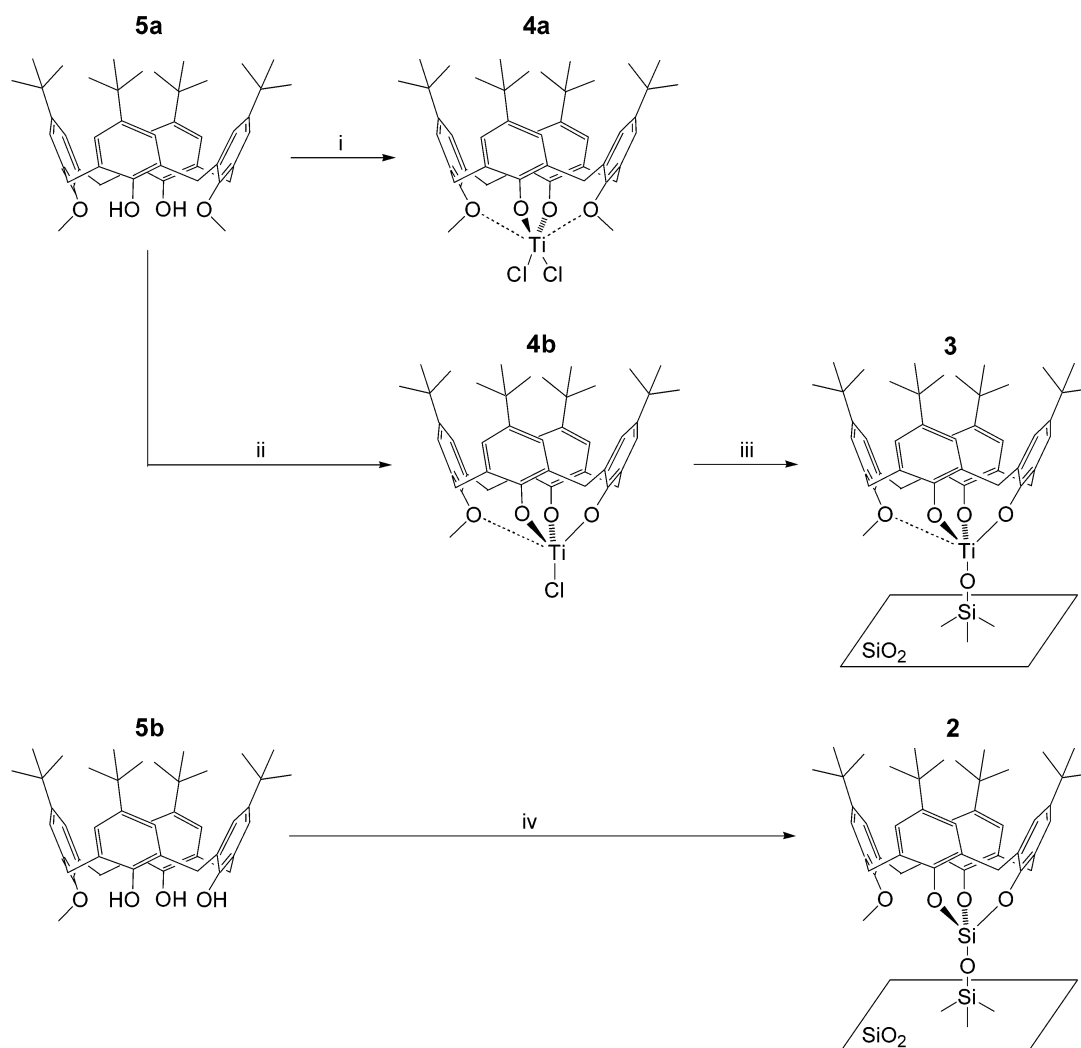
Immobilization of 5b To Yield 2-116. Using our previously published procedures,⁷ a suspension of 1.00 g of chlorinated silica gel was refluxed in 50 mL of toluene with 160 mg of **5b**²² (0.24 mmol) and 1.0 mL of NEt₃ (7.2 mmol, 2 equiv relative to surface silanols) to yield the silicon-containing analogue of **3**.

Catalysis. A 50 mg sample of catalyst (7 μmol of Ti for **3-138**) and ~300 mg of 4A or 3A molecular sieves were added to a 50 mL round-bottom flask with magnetic stirring. The reactor was sealed and degassed under dynamic vacuum at 25 °C for 1 h and at 70 °C for 1 h. The reactor was cooled under Ar backflow, charged with 40 mL of octane (solvent) and 6.5 mmol of substrate, sealed with a PTFE-coated rubber septum, and transferred to a 60 °C oil bath. After thermal equilibration, 1.5 mmol of *tert*-butyl hydroperoxide (TBHP; Fluka, ~5.5 M solution in nonane with 4A molecular sieves) or cumyl hydroperoxide (CHP; Fluka, ~80% solution in cumene, 4A molecular sieves added) was injected to start the reaction. Aliquots (100 μL) were removed periodically using a syringe, filtered to remove the catalyst, and analyzed using an Agilent 6890 GC system equipped with a flame ionization detector using an HP-1 methylsilicone capillary column. Cumene or nonane present in the hydroperoxide solution was used as an internal standard. Details of reagent purification and of product identification are given in the Supporting Information.

Analytical Characterization. Thermogravimetric analysis (TGA) was performed on a TA Instruments TGA 2950 system using a flow of dry synthetic air at a ramp rate of 5 °C/min. Carbon content was measured by the Berkeley Microanalytical Laboratory using a Perkin-Elmer 2400 Series II combustion analyzer. Titanium content was measured by Quantitative Technologies, Inc. using inductively coupled plasma mass spectrometry (ICP-MS).

- (11) Zanotti-Gerosa, A.; Solari, E.; Giannini, L.; Floriani, C.; Re, N.; Chiesi-Villa, A.; Rizzoli, C. *Inorg. Chim. Acta* **1998**, *270*, 298–311.
 (12) Saxton, R. J. *Top. Catal.* **1999**, *9*, 43–57.
 (13) Bellussi, G.; Rigutto, M. S. *Stud. Surf. Sci. Catal.* **1994**, *85*, 177–213.
 (14) Davis, M. E.; Katz, A.; Ahmad, W. R. *Chem. Mater.* **1996**, *8*, 1820–1839.
 (15) Davis, R. J.; Liu, Z. *Chem. Mater.* **1997**, *9*, 2311–2324.
 (16) Thomas, J. M. *Angew. Chem., Int. Ed.* **1999**, *38*, 3588–3628.
 (17) Gao, X.; Wachs, I. E. *Catal. Today* **1999**, *51*, 233–254.
 (18) Crocker, M.; Herold, R. H. M.; Orpen, A. G.; Overgaag, M. T. A. *J. Chem. Soc., Dalton Trans.* **1999**, 3791–3804.
 (19) Arends, I. W. C. E.; Sheldon, R. A. *Appl. Catal., A* **2001**, *212*, 175–187.
 (20) Hutter, R.; Mallat, T.; Baiker, A. *J. Catal.* **1995**, *153*, 177–189.
 (21) Wieser, C.; Dieleman, C. B.; Matt, D. *Coord. Chem. Rev.* **1997**, *165*, 93–161.

- (22) Groenen, L. C.; Ruël, B. H. M.; Casnati, A.; Verboom, W.; Pochini, A.; Ungaro, R.; Reinhoudt, D. N. *Tetrahedron* **1991**, *47*, 8379–8384.

Scheme 1. Precursor Synthesis and Grafting Procedures^a

^a Conditions: (i) **5a** with 1 equiv of TiCl_4 in toluene, 60 °C, 24 h, as synthesized by Radius;²⁷ (ii) reflux **5a** with 1 equiv of TiCl_4 in toluene, 48 h; (iii) reflux **4b** with partially dehydroxylated silica for 24 h in toluene with 10 equiv of 2,6 di-*tert*-butylpyridine; (iv) reflux **5b** with chlorinated silica for 24 h in toluene with 2 equiv of $\text{N}(\text{Et})_3$.

Spectroscopy. UV–vis spectroscopy was performed on a Varian Cary 400 Bio UV–vis spectrophotometer equipped with a Harrick Praying Mantis accessory for diffuse reflectance measurements on solids at room temperature. Compressed PTFE powders were used as a reference. Fluorescence spectra were measured using a Hitachi F-4500 fluorescence spectrophotometer with a solids reflectance accessory. Solid-state ^{13}C CP/MAS NMR was performed at the Caltech solid-state NMR facility using a Bruker DSX500 spectrometer operating at 500 MHz.

Results and Discussion

Materials Synthesis and General Characterization. The synthetic scheme for grafting metallocalixarenes is depicted in Scheme 1 and described in the Experimental Section. The catalyst synthesis can be generalized to the large library of upper- and lower-rim substituted calixarenes,²³ but care must be exercised to prevent the formation of multinuclear species.^{9,24,25} Precursor **4b** was immobilized with quantitative yield up to a surface density of 0.18 calixarene nm^{-2} (0.15 mmol g^{-1}). The surface density was increased to a maximum of 0.25

calixarene nm^{-2} (0.20 mmol g^{-1}) when an excess of **4b** was refluxed in the presence of silica for 280 h. After this point, additional **4b** had no effect on the ultimate surface coverage of **3** determined by TGA and elemental analysis. We note that the silanol density remains much higher than the calixarene active site density for all materials synthesized and is not appreciably changed upon calixarene grafting for silica pretreatment temperatures below 1000 °C.²⁶

A Ti atom:calixarene molecule ratio of 1.0 ± 0.1 was independently measured in **3** at all surface coverages (0.03–0.25 nm^{-2}) by combustion analysis and ICP-MS. These equimolar ratios strongly indicate that the molecular precursor **4b** was grafted intact. Bulk calixarene contents were estimated by total weight loss in TGA above 250 °C (Supporting Information Figure S1). The onset of weight loss upon heating **3** in air is quite dramatic, with a sharp maximum in the derivative plot centered between 360 and 380 °C. Calixarene

(23) Gutsche, C. D. *Calixarenes*; Royal Society of Chemistry: Cambridge, U.K., 1992.

(24) Clegg, W.; Elsegood, M. R. J.; Teat, S. J.; Redshaw, C.; Gibson, V. C. *J. Chem. Soc., Dalton Trans.* **1998**, 18, 3037–3039.

(25) Cotton, F. A.; Dikarev, E. V.; Murillo, C. A.; Petrukhina, M. A. *Inorg. Chim. Acta* **2002**, 332, 41–46.

(26) Zhuravlev, L. T. *Colloids Surf., A* **2000**, 173, 1–38.

Table 1. Summary of Materials Synthesized

ID	concn, $\mu\text{mol g}^{-1}$	pore vol, ^a cm^3/g	surface density, ^b calixarene nm^{-2}	[Ti], ^c wt %	Ti:calixarene
3	203	0.42	0.25	0.97	1.00
3	146	0.48	0.18	0.69	0.97
3	138	N/D	0.17	0.65	0.99
3	75	N/D	0.09	0.35	0.98
3	51	0.58	0.06	0.23	^d
3	25	N/D	0.03	0.11	^d
2	116	0.54	0.14		

^a The silica support has a pore volume of $0.69 \text{ cm}^3/\text{g}$. ^b Determined by combustion analysis. ^c Determined by ICP-MS. ^d A very low carbon content places large errors on the Ti:calix ratio. Nonetheless, values between 0.9 and 1.0 are always obtained.

contents were measured from combustion analysis and TGA, and both methods agreed to within 10%. Nitrogen physisorption data and BJH pore size distributions are similar to those reported previously for **17** and show decreasing total pore volume and average pore radius as calixarene loading is increased (Supporting Information Figure S2). The decrease in pore volume corresponds to an average calixarene–Ti^{IV} molecular volume of 2.3 nm^3 , in reasonable agreement with the molecular dimensions predicted from molecular models ($1.4 \text{ nm} \times 1.4 \text{ nm} \times 1.0 \text{ nm} = 2.0 \text{ nm}^3$). Additional materials characterization data are provided in Table 1.

Materials Spectroscopic Characterization. NMR spectroscopy provides additional compelling evidence that the atomic connectivity between Ti and calixarene in **3** is retained during grafting. Close comparison of ¹³C NMR spectra for materials **2** and **3** in the solid state and for molecular precursors **5a**²⁸ and **4a**²⁷ in deuterated chloroform shows that all four spectra are similar, with the exception of two resonances, 4 and 7'. In the spectra of the precursors, resonances 4 and 7' are shifted downfield 8 and 13 ppm, respectively, when Ti-containing **4a** is compared to unmetalated **5a**. Likewise, in the solid-state spectrum of **3**, resonances 4 and 7' are shifted by 2 and 11 ppm, respectively, relative to the resonances in **2** (Figure 1). These shifts are consistent with expected changes in electron density upon phenoxide (resonance 7') and methyl ether (resonance 4, inset) coordination to Ti. The latter coordination represents a weak dative bond inferred from interatomic distances between Ti and methyl ether oxygen in structures derived from single-crystal X-ray diffraction of **4a**,²⁷ **4b**,¹¹ and related titanocalixarenes.⁹ The resonance assignment for carbon 4 was verified by isotopically enriching the methoxy position in grafted calixarene materials.

UV–vis and fluorescence spectroscopies were used to probe the surface structures formed by grafting of **4b** onto silica. The absorption spectra of precursor **4b** and of immobilized **3** and **2** are shown in Figure 2A. All calixarenes exhibit an absorption maximum at 270–290 nm arising from π – π^* transitions, but only calixarene–Ti^{IV} complexes **3** and **4b** show an additional broad absorption feature at 290–500 nm, which we assign to calixarene–Ti^{IV} charge transfer (LMCT) bands. Material **6** was produced by treatment of **3** in dry air at 500 °C. This process removed all absorption features in the 290–500 nm range, confirming that these electronic transitions arise from the

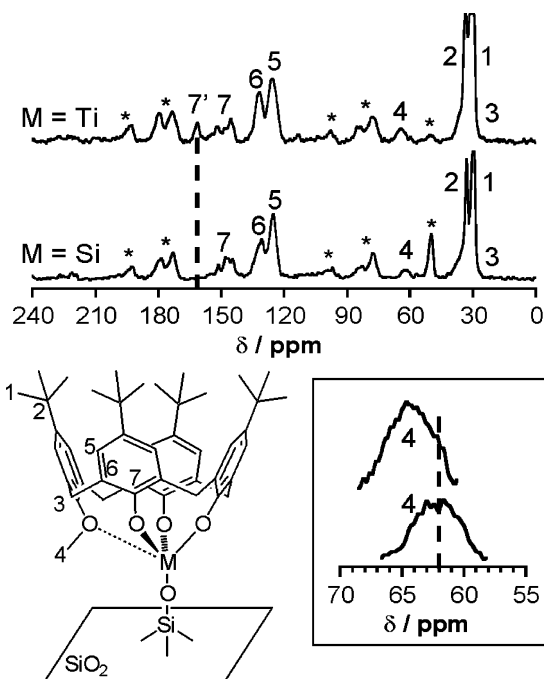


Figure 1. ¹³C CP/MAS NMR spectra of immobilized materials **2** (M = Si) and **3** (M = Ti). An asterisk indicates a spinning sideband or surface methoxide. The appearance of a distinct resonance 7' is indicative of phenoxide coordination to Ti. The inset highlights the downfield shift of resonance 4 in **3** relative to **2** due to methyl ether coordination to Ti.

calixarene ligands and also ruling out the presence of extended Ti–O–Ti connectivity²⁹ even after calcination. Fluorescence emission spectra ($\lambda_{\text{ex}} = 270 \text{ nm}$; Supporting Information Figure S3) of **3** show strong quenching relative to those of both the unmetalated calixarene **2** and the calcined **6**. This quenching is a common feature of d^0 metal–dye complexes,³⁰ and is consistent with Ti attachment to the calixarene in **3**.

We use the position of the calixarene–Ti^{IV} LMCT edge as a probe of catalyst structure, in much the same way as edge energies are used to characterize dispersed metal oxides.^{31,32} As seen in Figure 2B, extrapolation of the linear region to the intercept gives the same edge energy of $2.18 \pm 0.02 \text{ eV}$ (or 585 nm) for all grafted materials, irrespective of titanium loading. This strongly suggests that the structure of the predominant grafted species is independent of calixarene–Ti^{IV} surface density. In dispersed metal oxides, the edge energy is unchanged at low surface density, because of the predominant presence of isolated oxo species, and then decreases as metal centers become linked by bridging oxygens with increasing surface coverage.^{31,32} We attribute the constant edge energy in **3** up to the *maximum surface loading possible* to structural isolation enforced by the steric bulk of the calixarene and silica surface as ligands. The edge energy of the precursor molecule **4b** lies at 1.90 eV, 0.28 eV lower than that of the grafted **3**, reflecting the change of ligand from R_3SiO^- in **3** to Cl^- in **4b** and confirming that the Ti precursor has been covalently grafted, instead of merely physisorbed, on the surface.

(27) Radius, U. *Inorg. Chem.* **2001**, *40*, 6637–6642.

(28) ¹³C NMR (400 MHz, C_6D_6 , 298 K) δ 30.63, 31.84 ($\text{C}(\text{CH}_3)_3$), 32.25 (CH_2), 33.56, 33.85 ($\text{C}(\text{CH}_3)_3$), 62.79 (OMe), 125.58, 125.93 (Ar_m), 127.99, 132.34 (Ar_o), 141.20, 146.46 (Ar_p), 151.03, 151.63 (Ar_i).

(29) Guidotti, M.; Ravasio, N.; Psaro, R.; Ferraris, G.; Moretti, G. *J. Catal.* **2003**, *214*, 242–250.

(30) Rurack, K. *Spectrochim. Acta, Part A* **2001**, *57*, 2161–2195.

(31) Barton, D. G.; Shtein, M.; Wilson, R. D.; Soled, S. L.; Iglesia, E. *J. Phys. Chem. B* **1999**, *103*, 630–640.

(32) Gao, X.; Bare, S. R.; Fierro, J. L. G.; Banares, M. A.; Wachs, I. E. *J. Phys. Chem. B* **1998**, *102*, 5653–5666.

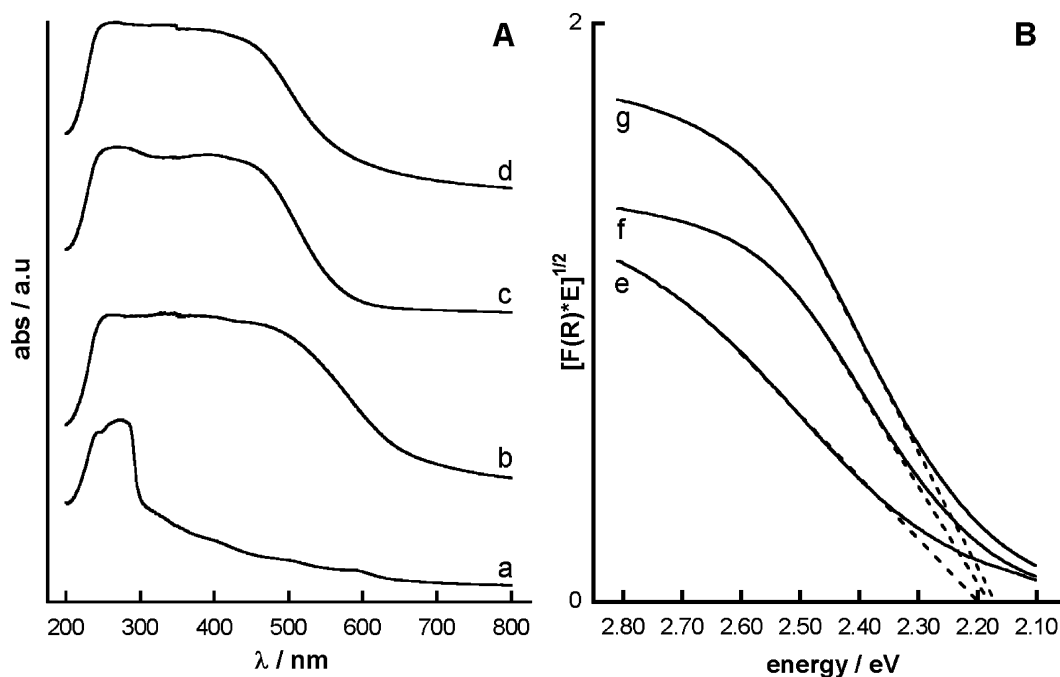


Figure 2. (A) UV-vis absorption spectra of (a) **2**, (b) **4b**, (c) **3**, and (d) **3** after 25 turnovers to cyclohexene epoxide at 60 °C, 10 min, CHP oxidant in octane. (B) Absorption edge region of representative catalysts (e) **3-51**, (f) **3-146**, and (g) **3-203**. Extending the linear region of each curve to the baseline gives an absorption edge energy of 2.18 ± 0.02 eV.

Table 2. Representative Epoxidation Results at 60 °C in Octane^a

no.	catalyst	oxidant	reactant	k_t^b M ⁻² s ⁻¹	TOF ₀ ^b h ⁻¹	conversion ^c			
						TON	%	time, h	
1	4b ^d	TBHP	cyclohexene	0.1	8	4	15	0.5	
2	3-25	TBHP	cyclohexene	11.0	181	633	54	8	
3	3-51	TBHP	cyclohexene	11.1	188	343	58	2	
4	3-75	TBHP	cyclohexene	10.8	195	367	92	5	
5	3-138	TBHP	cyclohexene	11.5	180	165	77	2	
6	3-146	TBHP	cyclohexene	11.0	181	156	83	2	
7	3-203	TBHP	cyclohexene	11.3	183	130	97	2	
8	3-51	CHP	cyclohexene	24.5	381	338	74	2	
9	3-146	CHP	cyclohexene	27.7	416	162	98	2	
10	3-203	CHP	cyclohexene	24.8	308	115	97	1	
11	3-138 ^e	CHP	cyclohexene	<i>f</i>	1080	202	98	0.5	
12	3-146	CHP	cyclooctene	<i>f</i>	690	170	99	1.3	
13	3-146	CHP	1-octene	0.5	7	42	22	4	
14	3-146	CHP	<i>cis</i> -stilbene	7.6	25	61	39	3	
Literature Comparisons									
15	TiCl ₄ ·SiO ₂ ⁴⁰	TBHP	cyclohexene	N/A	100	90	90	1.5	
16	CpTiSi ₇ O ₁₂ ·MCM-41 ⁴¹	TBHP	cyclooctene	N/A	202	1120	84	22	
17	Cp ₂ TiCl ₂ ·MCM-41 ³⁴	TBHP	cyclohexene	N/A	172	122	50	1	
18	dry TiO ₂ /SiO ₂ ⁴²	TBHP	cyclohexene	N/A	460	230	91	0.5	
19	TiO ₂ /SiO ₂ ²⁰	CHP	cyclohexene	N/A	540	72	82	1.5	
20	Ti(OSiR ₃) ₄ ·SBA-15 ⁴	CHP	cyclohexene	N/A	1500	600	98	2	

^a General reaction conditions are given in the Experimental Section. ^b k_t determined from $r = k[\text{cat}][\text{P}][\text{A}]$ based on the observed epoxide production rate. TOF₀ = (moles of epoxide/mole of Ti)/hour extrapolated to initial time. ^c Total conversion of peroxide at a given time. ^d A 5 μmol sample of **4b**, 5 mL of octane, and 0.65 mmol of cyclohexene. ^e Only 7 mL of octane used to increase all reactant concentrations. ^f Reaction was extremely rapid, and insufficient data could be collected to calculate a meaningful rate constant.

Catalytic Behavior of 3. Material **3** can be expected to be an active and selective epoxidation catalyst as a result of its rigid immobilization within a pseudotetrahedral geometry, which is often cited as a requirement for heterogeneous epoxidation catalysis on Ti centers.^{17,18,33–35} Epoxidation rates and selectivities for several unfunctionalized alkenes (Table 2) were

measured at 60 °C using CHP or TBHP as oxidants and dry octane as solvent. Material **3** catalyzes cyclohexene epoxidation with both TBHP and CHP; rates were slightly higher with CHP. Cyclohexene epoxidation on catalyst **3** typically proceeded to >95% conversion and >95% selectivity to the epoxide (based on hydroperoxide). Epoxidation of 1-octene on **3** and cyclohexene on **4b** occurs at a very low rate, and as such, unproductive thermal and surface-catalyzed decomposition of the hydroperoxide accounts for much of the total conversion, and the selectivity decreases to 30% and 66%, respectively.

(33) Abbenhuis, H. C. L. *Chem.—Eur. J.* **2000**, *6*, 25–32.

(34) Maschmeyer, T.; Rey, F.; Sankar, G.; Thomas, J. M. *Nature* **1995**, *378*, 159–162.

(35) Imamura, S.; Nakai, T.; Utani, K.; Kanai, H. *J. Catal.* **1996**, *161*, 495–497.

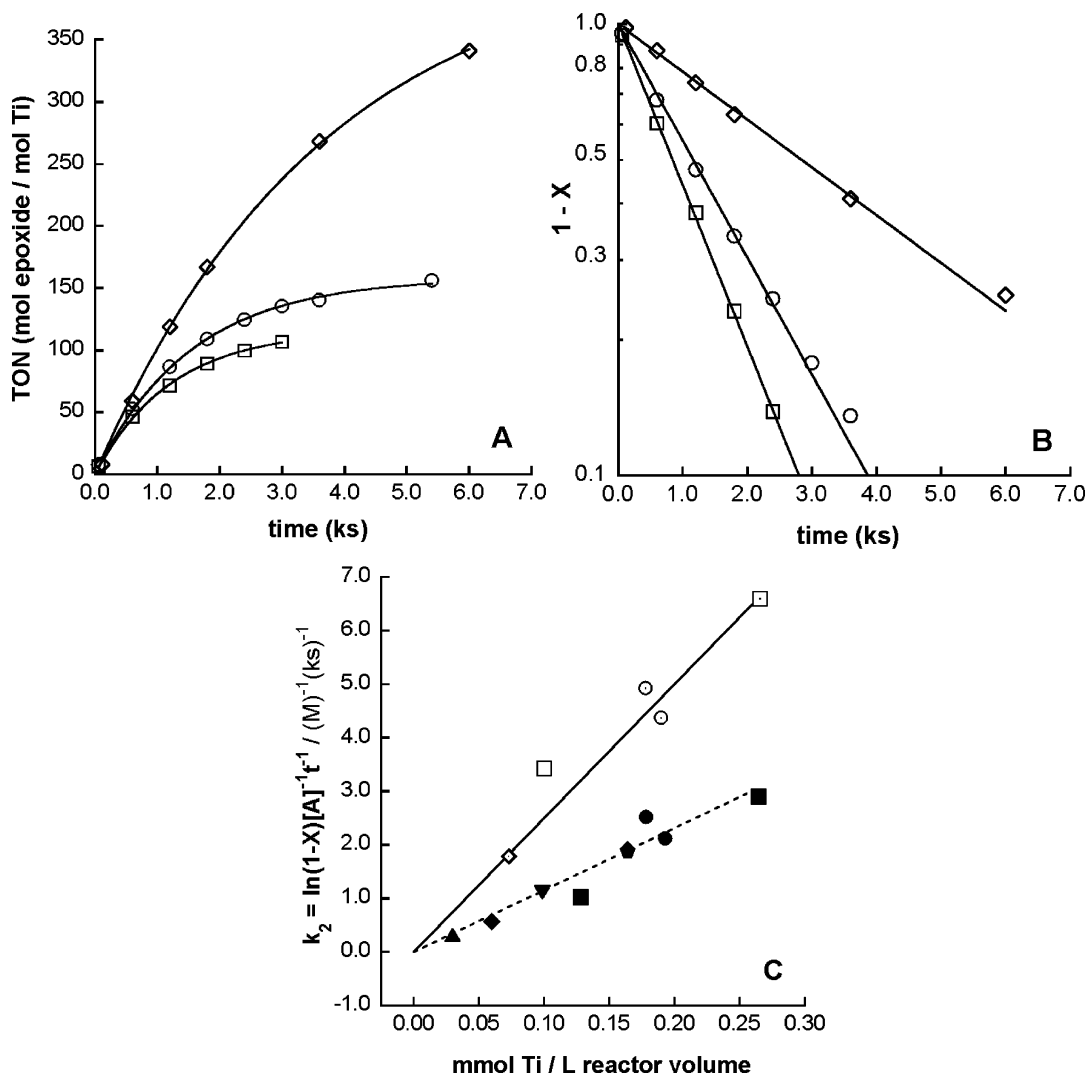


Figure 3. Cyclohexene epoxidation in octane at 60 °C catalyzed by **3**: (■□) **3**-203, (●○) **3**-146, (●) **3**-139, (▼) **3**-75, (◆◇) **3**-51, (▲) **3**-25. Open symbols are for CHP, and closed symbols are for TBHP. (A) TON to epoxide, CHP oxidant. Lines are fit using the first-order rate law proposed in the text. (B) Conversion X to epoxide, CHP oxidant. Lines are obtained by linear regression of the data points shown. The slope is proportional to the pseudo-first-order rate constant k_1 . (C) Second-order rate constants k_2 for CHP (—) and TBHP (---) plotted against total Ti concentration in the reactor. Lines are obtained by linear regression of the data points shown. The slope represents the intrinsic rate constant for epoxidation of cyclohexene with each oxidant.

Regardless, for all surface coverages and substrates, no side products (i.e., other C_6 oxides for cyclohexene) were detected by gas chromatography, essentially ruling out contributions from competing radical pathways.³⁶ Also, epoxidation of *cis*-stilbene proceeded with complete retention of configuration to only *cis*-stilbene oxide, which confirms that a nonradical mechanism is responsible for epoxidation in our catalysts.³⁷

The epoxidation of cyclooctene and 1-octene proceeded at the expected rates relative to those of cyclohexene. The observed relative substrate reactivity was cyclooctene > cyclohexene \gg 1-octene, consistent with attack of the alkene at an electrophilic coordinated peroxide oxygen.³⁸ The successful epoxidation of stilbene and cyclooctene indicates the absence of significant steric constraints at the active site.^{20,34,39}

Table 2 also shows that cyclohexene epoxidation rates on catalyst **3** resemble or exceed those reported on state-of-the-art

Ti-based heterogeneous epoxidation catalysts. Of particular note is the high TOF reported for entry 20. This material is a highly dispersed grafted species that provides good active site accessibility. However, as for other catalysts in Table 2, the TOF of the catalyst in entry 21 decreases as the surface density increases, suggesting that site isolation may be incomplete.⁴ We note that our reaction conditions are much more dilute than most in the literature using Ti-based catalysts; thus, rates reported here on material **3** underestimate those expected at the higher reactant concentrations of comparative studies.^{4,20,42}

Kinetic Analysis. Figure 3A shows catalytic turnovers to epoxide (TON = moles of epoxide/mole of Ti) in CHP and excess cyclohexene as a function of reaction time using **3** as catalyst at 60 °C. Figure 3B shows epoxide yields based on peroxide (X = moles of epoxide/initial mole of peroxide). Neither plot shows an induction period, indicating that the

(36) Figueras, F.; Kochkar, H. *Catal. Lett.* **1999**, *59*, 79–81.
 (37) Oldroyd, R. D.; Thomas, J. M.; Maschmeyer, T.; MacFaul, P. A.; Snelgrove, D. W.; Ingold, K. U.; Wayner, D. D. M. *Angew. Chem., Int. Ed. Engl.* **1996**, *35*, 2787–2790.
 (38) Sheldon, R. A. *J. Mol. Catal.* **1980**, *7*, 107–126.
 (39) Dartt, C. B.; Davis, M. E. *Appl. Catal., A* **1996**, *143*, 53–73.

(40) Sheldon, R. A.; van Doorn, J. A. *J. Catal.* **1973**, *31*, 427–437.
 (41) Krijnen, S.; Abbenhuis, H. C. L.; Hanssen, R. W. J. M.; Van Hooff, J. H. C.; van Santen, R. A. *Angew. Chem., Int. Ed.* **1998**, *37*, 356–358.
 (42) Corma, A.; Domine, M.; Gaona, J. A.; Jordá, J. L.; Navarro, M. T.; Rey, F.; Pérez-Parienta, J.; Tsuji, J.; McCulloch, B.; Nemeth, L. T. *Chem. Commun.* **1998**, 2211–2212.

grafted species are the resting state of the active catalyst and not merely precursors to active structures.⁴³ The data in Figure 3B show a linear dependence of $\log(1 - X)$ on time at all peroxide conversions, and the pseudo-first-order rate constants, proportional to the slope of these lines, are unaffected by increasing reaction time. These results indicate that catalyst deactivation, leaching, or inhibition by products do not occur. Consistent with this linear behavior, the deliberate addition of an excess of coproduct alcohol at initial time did not influence reaction rates or reactant conversions.

The lack of kinetic inhibition by alcohol products suggests a strong preference for binding peroxide reactants instead of abundant alcohol products on Ti active centers. First-order behavior was observed previously on Ti–silsesquioxane complexes⁴¹ and early Ti–SiO₂ catalysts,⁴⁰ but many initially active epoxidation catalysts deactivate with reaction time,^{4,18,34} an effect that has been ascribed to inhibition by alcohol products.

Grafted calixarene–Ti^{IV} catalysts reported here can be stored in ambient air without detectable changes in epoxidation rates and selectivities compared to freshly prepared materials. This stability is in marked contrast to the sensitivity of conventional Ti epoxidation catalysts to atmospheric moisture during storage, which causes irreversible restructuring around Ti centers. As with other epoxidation catalysts stable during storage, such as grafted Ti(OSiPh₃)₄,² traces of water during catalysis led to lower selectivities and rate constants with increasing reaction time, apparently as a result of acid-catalyzed epoxide hydrolysis, which forms chelating diols that bind strongly to Ti centers.⁴² This situation is avoided by conducting the reaction in the presence of molecular sieves,^{44,45} as we have performed here.

Experimental Evidence for Single-Site Behavior. Silica gel surfaces are known to exhibit a distribution of acid sites, and this can influence the number and type of ligands at a grafted metal center.⁴⁶ In contrast, we expect the bonding around the Ti center in **3** to be largely controlled by the multidentate calixarene ligand, which should force the Ti into a pseudotetrahedral coordination geometry, as in the single-crystal X-ray diffraction structure of precursor **4b**.¹¹ To test this hypothesis, we examined the epoxidation of cyclohexene using **3** as catalyst, with a wide range of surface concentrations of Ti active sites from 0.03 to 0.25 nm⁻².

Catalytic activity in a single-site material depends only on the total concentration of Ti centers and not their surface concentration. In Figure 3A, turnover frequencies for cyclohexene epoxidation (TOF = TON/time) extrapolated to initial times show identical TOFs (slope) on catalysts with surface densities between 0.06 and 0.25 nm⁻². This behavior is usually considered sufficient to prove single-site behavior,⁴ but here we compare rate constants over the entire time course of reaction to unequivocally prove the single-site behavior of **3** as catalyst.

In view of the linearity of the conversion data when plotted as $\log(1 - X)$ and the large excess of cyclohexene reactants used, we use a rate law given by $r = k[\text{cat}][\text{P}][\text{A}]$, where [P] is the concentration of hydroperoxide (mol/L) and [A] is the concentration of alkene (mol/L), which is essentially unchanged

during reaction. The first-order dependence on hydroperoxide was established above, and the dependence on alkene was verified independently. At the reaction conditions given in the Supporting Information, the initial TOF increased linearly from 34 to 65 to 160 h⁻¹ as the cyclohexene concentration was raised from 18 to 48 to 138 mM (Supporting Information Figure S4). The final concentration is approximately that of the reaction system employed in this paper. The catalyst concentration [cat] is expressed as millimoles of Ti per reactor volume (L). The rate was obtained from the integrated form of the rate expression $\ln(1 - X) = k[\text{cat}][\text{A}]t = k_2[\text{A}]t = k_1t$. A graph of $\ln(1 - X)[\text{A}]^{-1}$ versus time has a slope of k_2 and a zero intercept. A plot of k_2 as a function of [cat] (Figure 3C) leads to a straight line through the origin for single-site materials and a curve of decaying slope for conventional grafted Ti catalysts.^{4,32,47}

The value of k_2 was determined for each catalyst using this methodology, and the linear dependence shown by the data in Figure 3C unequivocally shows that intrinsic rate constants depend only on the number of Ti centers in the reactor and not on the calixarene–Ti^{IV} surface coverage, an accepted hallmark of single-site catalysts. Also, the use of intrinsic rate constants instead of initial TOF ensures that these materials behave identically at all conversions, rather than only during initial contact with reactants. The rate constants k in Figure 3C are $11.1 \pm 0.3 \text{ M}^{-2} \text{ s}^{-1}$ for TBHP and $25 \pm 2 \text{ M}^{-2} \text{ s}^{-1}$ for CHP over the entire range of calixarene–Ti^{IV} surface coverages (0.03–0.25 nm⁻²).

This demonstrated single-site behavior differs markedly from that reported on other Ti-based catalysts, for which epoxidation turnover rates (per Ti center) either decrease monotonically with increasing Ti concentration^{4,32,47} or sharply decrease above a certain value,^{12,13,20} apparently because metal centers increasingly reside at inactive or inaccessible surface sites or because oligomers form with less active and selective Ti–O–Ti connectivity. We propose that the steric bulk and geometric constraints provided by the calixarene ligand prevent metal center clustering or nonuniform coordination geometries even near saturation coverage.

Identification of Catalytically Relevant Species. Control experiments first sought to confirm the heterogeneous nature of the catalysis observed and to determine the stability of **3** against leaching during reaction. The homogeneous precursor **4b**⁴⁴ (Table 2, entry 1) and its *tert*-butoxy analogue showed >20-fold lower activity than the grafted material **3**. The addition of pure silica to a reaction mixture containing homogeneous material **4b** synthesizes **3** in situ, as determined by TGA and UV–vis spectroscopy of recovered solids, and leads to a concomitant increase in epoxidation rates (Supporting Information Figure S5a). This illustrates the importance of Ti–O–Si connectivity for epoxidation catalysis^{18,33} and demonstrates synergy between grafted precursors and the support.

In several experiments, a reaction mixture of catalyst **3**–138, CHP, and cyclohexene was filtered at 60 °C after reaction for 10 min (TON \approx 30). The filtrate showed no detectable epoxidation activity over 1 h (Figure S5b). Also, the addition of pure silica to the filtrate, a procedure that leads to in situ immobilization of **3** and to the appearance of catalytic activity

(43) Schofield, L. J.; Kerton, O. J.; McMorn, P.; Bethell, D.; Ellwood, S.; Hutchings, G. J. *J. Chem. Soc., Perkin Trans. 2* **2002**, 1475–1481.

(44) Massa, A.; D'Ambrosi, A.; Pronto, A.; Scettri, A. *Tetrahedron Lett.* **2001**, *42*, 1995–1998.

(45) Dusi, M.; Mallat, T.; Baiker, A. *J. Catal.* **1998**, *173*, 423–432.

(46) Lefort, L.; Chabanas, M.; Maury, O.; Meunier, D.; Copéret, C.; Thivolle-Cazat, J.; Basset, J. M. *J. Organomet. Chem.* **2000**, *593–594*, 96–100.

(47) Ikeue, K.; Ikeda, S.; Watanabe, A.; Ohtani, B. *Phys. Chem. Chem. Phys.* **2004**, *6*, 2523–2528.

when homogeneous **4b** is present in solution, did not lead to detectable epoxidation products after an additional 1 h at 60 °C.

The absence of leaching cannot be demonstrated unequivocally from the observed noncatalytic character of the filtrate because of the low epoxidation rates on homogeneous catalyst **4b** and on its *tert*-butoxy analogue. Recycle experiments (Figure S5c), in which the catalyst is washed with hot anhydrous octane, dried, weighed, and used for another catalytic cycle, showed very similar reaction rates and conversions in subsequent catalytic runs (within 5%), confirming the absence of permanent deactivation or leaching of sites. Also, addition of a second aliquot of hydroperoxide after 100% conversion (Figure S5d) led to an identical conversion rate, confirming that the catalyst remains active in the presence of all reaction products and is not, perhaps, reactivated by the recycling process.

Analysis of the solids recovered after filtration also did not detect elemental or structural changes indicative of leaching of calixarenes or of Ti-containing species. TGA and Ti ICP-MS independently did not detect changes in the carbon or titanium content within their respective accuracies (~5%). UV-vis spectroscopy (Figure 2A) and ¹³C CP/MAS NMR (Supporting Information Figure S6) of the solids recovered after catalysis showed that **3** was essentially unaltered during reaction. When catalysis was deliberately performed under deactivating conditions (without molecular sieves), the loss in activity was paralleled by a loss in calixarene content by both UV-vis and ¹³C CP/MAS NMR of the solids (Figure S6). In the ¹³C CP/MAS NMR experiment, aromatic calixarene resonances were replaced by alkoxide resonances. These data, coupled with an unchanged Ti content by ICP-MS, suggest that diol formation from epoxide hydrolysis leads to the displacement of the calixarene ligand with concomitant loss of catalytic activity.

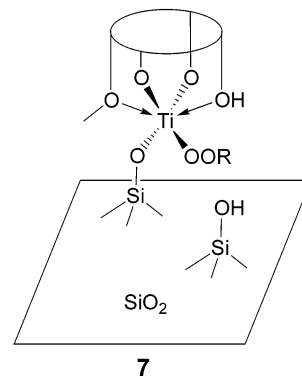
Deliberate calixarene removal by combustion in dry air at 500 °C produces catalyst **6-146**, which shows behavior essentially similar to that of the grafted and calcined titanocene catalyst reported by Maschmeyer et al.³⁴ Under identical conditions,

the initial epoxide TOF on **6-146** was 504 h⁻¹ as compared to 416 h⁻¹ on **3-146**, but unlike the grafted calixarene catalyst, epoxide production essentially stopped at an 80% yield of epoxide. After this point, peroxide consumption continued and a small fraction of the epoxide was decomposed (likely to ring-opened product). At identical conditions, catalyst **3** continued to >98% conversion with 100% selectivity. The relative increase in initial TOF for **6-146** presumably reflects the removal of steric limitations around the Ti center imposed by the calixarene ligand. At high conversions, the absence of a calixarene ligand results in strong inhibition by coproduct alcohol, as reported previously.³⁴

Taken together, these results indicate that material **3** is stable with respect to ligand loss and does not leach into solution as less active homogeneous species, such as titanium alkoxides, which can potentially form during reaction. We conclude, therefore, that the immobilization of active species **3** is permanent under the conditions reported here and that it is required for efficient and selective epoxidation catalysis.

Proposed Reaction Intermediate. We propose here structure **7** for the active species as consistent with catalytic and characterization data, but we note that the bonding mode of the

Ti-peroxide intermediate in heterogeneous epoxidation catalysis remains unclear.^{48–51}



The bound peroxide may be hydrogen-bonded with adjacent calixarene phenols or surface silanols as proposed for epoxidation in the presence of polar protic species,⁵⁰ or the intermediate could be an η^2 complex as proposed for the active site in grafted complexes⁵¹ and observed in model compounds.⁵² Also, while we cannot rule out insertion of the peroxide into the Ti–OSi bond,^{4,18,49} we believe that insertion into one of the Ti–OC bonds is more likely. Ti–OC bonds have been previously shown to be more kinetically labile than Ti–OSi bonds in the presence of TBHP.⁵ Particular to our system, the three-fold multiplicity of Ti–OC bonds relative to a single Ti–OSi bond favors the proposed structure **7**, and cleavage of a Ti–OC bond will be further favored by release of conformational strain in the metallocalixarene. This strain is apparent in the elliptical conformation of the calixarene macrocycle in the structure of **4b** as determined by single-crystal X-ray diffraction.¹¹ Finally, **7** maintains the Ti–OSi connection required for the observed heterogeneous catalysis.

Many factors, including steric constraints at the metal,^{18,33,53} diffusion to the active site,^{20,39,54} and support hydrophobicity,^{36,42,55} influence epoxidation catalysis on Ti centers, but alkene epoxidation rates are expected to increase with increasing electron-withdrawing power of oxo ligands.⁴⁰ In this context, the main role of the calixarene ligand in **3** in epoxidation catalysis is to withdraw electron density from the peroxide oxygens in a reaction intermediate such as **7**, rendering such oxygens more electrophilic and prone to alkene attack.

We suggest that calixarene ligands in **3** perform two simultaneous functions by (i) introducing steric constraints that prevent dimerization and formation of weaker Ti–O–Ti Lewis acids^{18,34,56} and (ii) promoting Lewis acidity at the Ti center

- (48) Bonino, F.; Damin, A.; Ricchiardi, G.; Ricci, M.; Spanò, G.; D'Aloisio, R.; Zecchina, A.; Lamberti, C.; Prestipino, C.; Bordiga, S. *J. Phys. Chem. B* **2004**, *108*, 3573–3583.
- (49) Sinclair, P. E.; Catlow, C. R. A. *J. Phys. Chem. B* **1999**, *103*, 1084–1095.
- (50) Bellussi, G.; Carati, A.; Clerici, M. G.; Maddinelli, G.; Millini, R. *J. Catal.* **1992**, *133*, 220–230.
- (51) Adam, W.; Corma, A.; García, H.; Weichold, O. *J. Catal.* **2000**, *196*, 339–344.
- (52) Boche, G.; Möbus, K.; Harms, K.; Marsch, M. *J. Am. Chem. Soc.* **1996**, *118*, 2770–2771.
- (53) Klunduk, M. C.; Maschmeyer, T.; Thomas, J. M.; Johnson, B. F. G. *Chem.—Eur. J.* **1999**, *5*, 1481–1485.
- (54) Blasco, T.; Corma, A.; Navarro, M. T.; Pariente, J. P. *J. Catal.* **1995**, *156*, 65–74.
- (55) Müller, C. A.; Deck, R.; Mallat, T.; Baiker, A. *Top. Catal.* **2000**, *11/12*, 369–378.
- (56) Sarsfield, M. J.; Ewart, S. W.; Tremblay, T. L.; Roszak, A. W.; Baird, M. C. *J. Chem. Soc., Dalton Trans.* **1997**, 3097–3104.

relative to conventional alkoxide⁵⁷ or Cp⁵⁶ ligands. This stronger Lewis acidity reflects the effective delocalization of electron density away from the Ti center via Ti–O–Ph π -bonding;¹¹ this mechanism is analogous to that invoked for the increased Lewis acidity in early-transition-metal complexes with siloxy ligands relative to those with alkoxy ligands.^{57–59} A similar argument has also been invoked for the high activity and stability of grafted transition-metal alkyls as polymerization catalysts.⁶⁰

Conclusions

We demonstrate here a novel route for the synthesis of isolated Ti–oxo complexes via grafted metallocalixarenes and their use as highly active and selective epoxidation catalysts. The single-site nature of the observed electronic transitions and catalysis on these materials confirms our premise that the steric bulk of calixarene ligands prevents oligomerization events leading to inactive and unselective Ti–O–Ti structures. The coordination environment enforced by the cone calixarene ligand leads to strong Lewis acidity and to faster epoxidation rates compared with those in conventional Ti centers with alkoxy and Cp ligands. The calixarene ligand provides steric constraints around each Ti center, which leads to remarkable stability during ambient storage and epoxidation catalysis, as well as to 100% selectivity to epoxide products. We expect this to be a general

method for creating surface organometallic species since we have shown that the calixarene–Ti^{IV} connectivity has been maintained from the crystallographically characterized precursor to the active catalytic species. We are currently exploiting the diversity and flexibility made available by calixarene ligands and the possibility of modifying the support properties for additional improvements in epoxidation rates and selectivities on grafted metallocalixarene materials.

Acknowledgment. We acknowledge the Exxon-Mobil Foundation and the University of California at Berkeley, Department of Chemical Engineering for financial support. J.M.N. is grateful to the National Science Foundation for a graduate fellowship. A.K. acknowledges the receipt of a Hellman Family Faculty Award and a 3M Pre-Tenure Faculty Award. We acknowledge Dr. Sonjong Hwang at the Caltech solid-state NMR facility for his technical assistance.

Supporting Information Available: Catalysis method and substrate purification details, characteristic TGA of **3-146** (Figure S1), characteristic nitrogen physisorption data (Figure S2), characteristic fluorescence emission spectra (Figure S3), investigation of reaction order in alkene concentration (Figure S4), silica addition (Figure S5a), filtration (Figure S5b), recycle (Figure S5c), and second aliquot (Figure S5d) catalysis experiments, and UV–vis (Figure S6a) and ¹³C NMR (Figure S6b) comparison for fresh, active, and deactivated catalysts. This material is available free of charge via the Internet at <http://pubs.acs.org>.

JA0470259

(57) Coffindaffer, T. W.; Steffy, B. D.; Rothwell, I. P.; Foltz, K.; Huffman, J. C.; Streib, W. E. *J. Am. Chem. Soc.* **1989**, *111*, 4742–4749.

(58) LaPointe, R. E.; Wolczanski, P. T.; Van Duyne, G. D. *Organometallics* **1985**, *4*, 1810–1818.

(59) Rice, G. L.; Scott, S. L. *Langmuir* **1997**, *13*, 1545–1551.

(60) Ballard, D. G. H.; Heap, N.; Kilbourn, B. T.; Wyatt, R. J. *Makromol. Chem.* **1973**, *170*, 1–9.